Inorganic Chemistry
Article

Inorg. Chem. **2010**, *49*, 1363–1371 **1363**
DOI: 10.1021/ic9010899

Recognition of Some Lanthanides, Actinides, and Transition- and Heavy-Metal Cations by N-Donor Ligands: Thermodynamic and Kinetic Aspects

Véronique Hubscher-Bruder,* Jaouad Haddaoui, Saliha Bouhroum,† and Françoise Arnaud-Neu*

Laboratoire de Chimie Physique, IPHC-DSA, UDS, CNRS, ECPM, 25 rue Becquerel, 67087 Strasbourg Cedex 2, France. †Deceased in September 2008.

Received June 5, 2009

The remarkable actinide(III) selectivity of the polyaromatic N-donors bis-triazine-pyridines (BTPs), *hemi*-bis-triazine-pyridines (*hemi*-BTPs) and bis-triazine-bipyridines (BTBPs) make these ligands the most promising candidates in partitioning and transmutation processes developed so far to better manage nuclear waste. The interactions of *n*-Pr-BTP, C_5-*hemi*-BTP, and the two most extensively investigated BTBPs (C_5-BTBP and $CyMe_4$-BTBP) have been studied with some representative lanthanide(III), uranyl, thorium, and transition- and other heavy-metal cations in methanol. The formation of complexes of different stoichiometries, the stability of which depended on both the ligands and the cations, was shown using UV absorption spectrophotometry. Study of the complexation reactions of La^{3+}, Eu^{3+} and Yb^{3+} with these four ligands by stopped-flow spectrophotometry allowed determination of the rate constants and postulation of possible complexation mechanisms.

Introduction

For many years, efforts have been made to develop improved procedures for the management of wastes from nuclear power plants. A strategy to reduce the volume and storage time of nuclear waste is partitioning and transmutation (P&T), which leads to less radiotoxic and shorter-lived radionuclides. In the SANEX process, long-lived trivalent minor actinides (An(III), such as americium and curium) are separated from trivalent lanthanides (Ln(III), present in large excess) using selective extractants before they are transmuted. This step is necessary to improve the efficiency of neutron irradiation of actinides, which have neutron capture cross sections smaller than those of the lanthanides. To perform the partitioning, complexing molecules have to be designed to discriminate between Ln(III) and An(III). This is not an easy task, because of the very similar chemical properties of these two series of elements. However, it has been shown that soft N and S donor ligands have a preference for Am(III) over Eu(III).[1] Efficient extraction agents have been synthesized in the past (bis(chlorophenyl)dithiophosphinic acid, thiomalonamides, thioglycolamides) but completely incinerable molecules containing only C, H, O, and N are preferred to avoid secondary waste generation.[2,3] Among the molecules recently studied to perform An(III)/Ln(III) separation, polyaromatic N-donor ligands of the bis-triazine-pyridine (BTP), *hemi*-bis-triazine-pyridine (*hemi*-BTP) and bis-triazine-bipyridine (BTBP) types have shown interesting binding properties and selectivity toward An(III). The first-studied tridentate BTPs showed good extraction properties without the addition of a synergist, but their poor radiolysis and hydrolysis stability was not compatible with an industrial application.[4] *Hemi*-BTPs whose chemical properties are similar to those of terpy have also been shown to be unstable in acidic media. The tetradentate BTBPs containing an additional pyridine group present many advantages: they have a better solubility in a wide range of solvents, they are good extractants, they allow the stripping of the extracted cations, and they show greater stability toward hydrolysis and radiolysis.[4−10] However,

*To whom correspondence should be addressed. E-mail: veronique.hubscher@unistra.fr (V.H.-B.); farnaud@chimie.u-strasbg.fr (F.A.-N.).

(1) Dam, H. H.; Reinhoudt, D. N.; Verboom, W. *Chem. Soc. Rev.* **2007**, *36*, 367–377.
(2) Kolarik, Z. *Chem. Rev.* **2008**, *108*, 4208–4252.
(3) Madic, C.; Testard, F.; Hudson, M. J.; Liljenzin, J.-O.; Christiansen, B.; Ferrando, M.; Facchini, A.; Geist, A.; Modolo, G.; Gonzales-Espartero, A.; De Mendoza, J. *PARTNEW, Final Report, CEA-R-6066*; CEA-Valrho, Marcoule, France, **2004**.
(4) Ekberg, C.; Fermvik, A.; Retegan, T.; Skarnemark, G.; Foreman, M. R. S.; Hudson, M. J.; Englund, S.; Nilsson, M. *Radiochim. Acta* **2008**, *96*, 225–233.
(5) Drew, M. G. B.; Foreman, M. R. S. J.; Hill, C.; Hudson, M. J.; Madic, C. *Inorg. Chem. Commun.* **2005**, *8*, 239–241.
(6) Nilsson, M.; Andersson, S.; Drouet, F.; Ekberg, C.; Foreman, M.; Hudson, M.; Liljenzin, J.-O.; Magnusson, D.; Skarnemark, G. *Solv. Extr. Ion Exch.* **2006**, *24*, 299–318.
(7) Nilsson, M.; Ekberg, C.; Foreman, M.; Hudson, M.; Liljenzin, J.-O.; Modolo, G.; Skarnemark, G. *Solv. Extr. Ion Exch.* **2006**, *24*, 823–843.
(8) Geist, A.; Hill, C.; Modolo, G.; Foreman, M.R.St.J.; Weigl, M.; Gompper, K.; Hudson, M. J. *Solv. Extr. Ion Exch.* **2006**, *24*, 463–483.
(9) Hudson, M. J.; Boucher, C. E.; Braekers, D.; Desreux, J. F.; Drew, M. G. B.; Foreman, M. R. St. J.; Harwood, L. M.; Hill, C.; Madic, C.; Marken, F.; Youngs, T. G. A. *New J. Chem.* **2006**, *30*, 1171–1183.
(10) Retegan, T.; Ekberg, C.; Englund, S.; Fermvik, A.; Foreman, M. R. S.; Skarnemark, G. *Radiochim. Acta* **2007**, *95*, 637–642.

Published on Web 01/07/2010

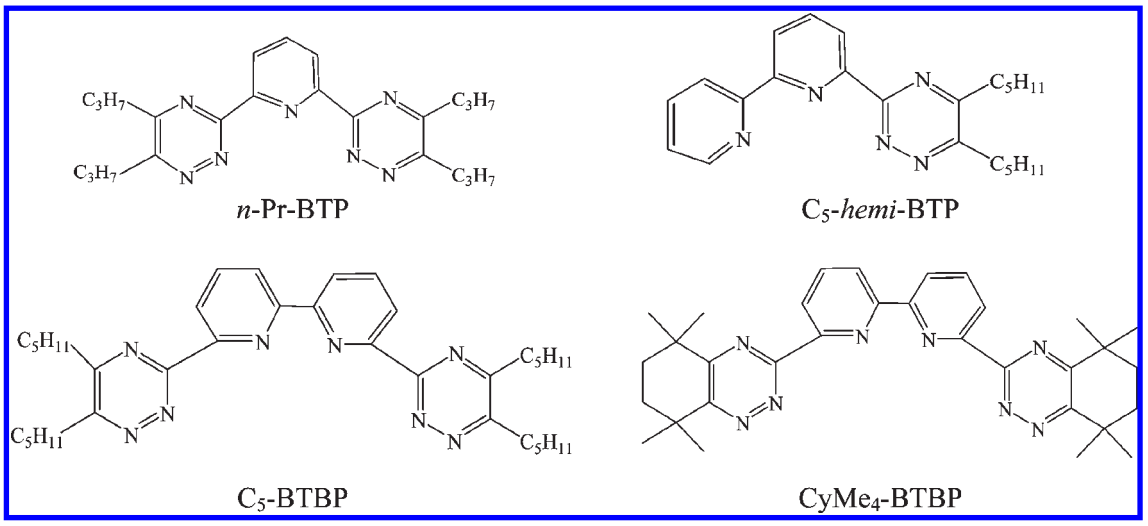

Figure 1. Chemical structure of the compounds studied in this work.

some previous works reported the affinity of these molecules for transition- and heavy-metal cations which could compete with An(III) during the extraction process.[11−14]

To design large-scale separation processes, the kinetics of separation has to be taken into account. In the case of $CyMe_4$-BTBP and some BTPs, it has been found that slow extraction and stripping kinetics can be accelerated by adding a phase transfer catalyst or by modifying the experimental conditions.[8,15]

Several studies have described the binding properties of these ligands in terms of stoichiometries and structure of the complexes formed, but few data are available on the stability constants of the complexation of Ln(III) and An(III) by N-containing molecules in homogeneous media. To our knowledge, no kinetic study has been performed yet on these systems in a common medium.

The present work focuses on the determination of thermodynamic parameters of the complexation of six lanthanides (La^{3+}, Nd^{3+}, Eu^{3+}, Gd^{3+}, Er^{3+}, and Yb^{3+}) and two actinides (Th^{4+}, UO_2^{2+}) by one BTP (2,6-bis(5,6-dipropyl-1,2,4-triazin-3-yl)pyridine, *n*-Pr-BTP), one *hemi*-BTP (6-(5,6-dipentyl-1,2,4-triazin-3-yl)-2,2′-bipyridine, C_5-*hemi*-BTP) and the two most extensively studied BTBPs (6,6′-bis(5,6-dipentyl-1,2,4-triazin-3-yl)-2,2′-bipyridine, C_5-BTBP; 6,6′-bis(5,5,8,8-tetramethyl-5,6,7,8-tetrahydrobenzo-1,2,4-triazin-3-yl)-2,2′-bipyridine, $CyMe_4$-BTBP) shown in Figure 1. As a first step, it is important to acquire basic knowledge on the coordination chemistry of these ligands with Ln(III) to better understand the interactions with these cations and to use them as surrogates for An(III). The binding properties of these ligands toward three transition-metal (Ni^{2+}, Cu^{2+}, Zn^{2+}) and five heavy-metal (Ag^+, Pb^{2+}, Cd^{2+}, Hg^{2+}, Tl^+) cations were also investigated. The results of a kinetic study are presented, and mechanisms for the recognition of La^{3+}, Eu^{3+}, and Yb^{3+} by these four ligands are proposed.

Experimental Section

Materials. The solvent methanol-Chromasolv (Sigma-Aldrich, maximum 0.03% water) was used without any further purification. The supporting electrolyte Et_4NNO_3 (Acros, 99%) was dried under vacuum for 24 h at room temperature. The following metal salts were used: $La(NO_3)_3 \cdot 6H_2O$, $Nd(NO_3)_3 \cdot H_2O$, $Eu(NO_3)_3 \cdot H_2O$, $Gd(NO_3)_3 \cdot H_2O$, and $Yb(NO_3)_3 \cdot xH_2O$ (Alfa Aesar, 99.99%); $Er(NO_3)_3 \cdot 5H_2O$ (Acros, 99.9%); $Th(NO_3)_4 \cdot 5H_2O$, $UO_2(NO_3)_2 \cdot 6H_2O$, $Ni(NO_3)_2 \cdot 6H_2O$, $Zn(NO_3)_2 \cdot 4H_2O$, $Pb(NO_3)_2$, and $Cd(NO_3)_2 \cdot 4H_2O$ (Merck, 99%); $Cu(NO_3)_2 \cdot 3H_2O$ (Prolabo, 99%); $AgNO_3$ (Acros, 99.85%); $Hg(NO_3)_2 \cdot H_2O$ (Fluka, puriss); $TlNO_3$ (Pierce Inorganics BV, 99%). All these salts were also dried under vacuum before use. The stock solutions of all of them except uranyl were standardized by complexometric titrations with EDTA.[16]

Potentiometry. The acid−base behavior of C_5-BTBP and C_5-*hemi*-BTP was studied potentiometrically. The concentration of free hydrogen ions was measured using a combined glass electrode (Mettler Toledo S7/120) connected to an automatic titrator (Metrohm Titrino DMS 716) at 25 °C. The standard filling solution of the external reference compartment of the electrode was replaced by a 0.01 M Et_4NCl solution in methanol saturated with AgCl. The electrode was calibrated by titration of a solution of 1.5×10^{-4} M $HClO_4$ with a Et_4NOH solution, previously standardized by potassium hydrogen phthalate. The parameters of the electrode in methanol were determined with the program SIRKO.[17] A 10 mL portion of a 10^{-3} M ligand solution was titrated with Et_4NOH at 25 °C under an atmosphere of argon ($I = 10^{-2}$ M in Et_4NNO_3). For each determination, at least two experiments were performed. The data were analyzed using the program Hyperquad.[18] The autoprotolysis constant of methanol used for the calculation was $pK_{MeOH} = 16.7$.[19]

Thermodynamic Study. UV Absorption Spectrophotometry. The stability constants β, equal to the molar ratio $[M_xL_y^{xn+}]/[M^{n+}]^x[L]^y$ (M^{n+} = cation, L = ligand), were determined by UV absorption spectrophotometry at 25.0 ± 0.1 °C in methanol and

(11) Foreman, M. R. St. J.; Hudson, M. J.; Geist, A.; Madic, C.; Weigl, M. *Solv. Extr. Ion Exch.* **2005**, *23*, 645–662.
(12) Ryu, J. Y.; Lee, J. Y.; Choi, S. H.; Hong, S. J.; Kim, C.; Kim, Y.; Kim, S.-J. *Inorg. Chim. Acta* **2005**, *358*, 3398–3406.
(13) Drew, M. G. B.; Foreman, M. R. St. J.; Geist, A.; Hudson, M. J.; Marken, F.; Norman, V.; Weigl, M. *Polyhedron* **2006**, *25*, 888–900.
(14) Ekberg, C.; Dubois, I.; Fermvik, A.; Retegan, T.; Skarnemark, G.; Drew, M. G. B.; Foreman, M. R. S.; Hudson, M. J. *Solv. Extr. Ion Exch.* **2007**, *25*, 603–617.
(15) Weigl, M.; Geist, A.; Müllich, U.; Gompper, K. *Solv. Extr. Ion Exch.* **2006**, *24*, 845–860.
(16) *Methodes d'analyses complexométriques par les Titriplex*, 3rd ed.; E. Merck AG: Darmstadt, Germany, 1992.
(17) Vetrogon, V. I.; Lukyanenko, N. G.; Schwing-Weill, M.-J.; Arnaud-Neu, F. *Talanta* **1994**, *41*, 2105–2112.
(18) Gans, P.; Sabatini, A.; Vacca, A. *Talanta* **1996**, *43*, 1739–1753.
(19) Tremillon, B. *La chimie en solvant non aqueux*; PUF: Paris, 1971.

Table 1. Stoichiometries (M:L) and Overall Stability Constants (log β)[a] for Lanthanide and Actinide Complexes with C_5-*hemi*-BTP, n-Pr-BTP, and BTBPs in Methanol ($I = 10^{-2}$ M, Et_4NNO_3; $T = 25$ °C)

	species M:L	La^{3+}	Nd^{3+}	Eu^{3+}	Gd^{3+}	Er^{3+}	Yb^{3+}	Th^{4+}	UO_2^{2+}
n-Pr-BTP	1:1	3.7 ± 0.1	n.d.[b]		n.d.	n.d.		n.d.	n.d.
	1:2			9.5 ± 0.03			10.3 ± 0.1		
	1:3			14.2 ± 0.2			14.3 ± 0.2		
C_5-*hemi*-BTP	1:1	2.8 ± 0.1	3.01 ± 0.02	3.6 ± 0.1	3.6 ± 0.1	4.18 ± 0.04	4.19 ± 0.08	3.9 ± 0.1	3.6 ± 0.2
C_5-BTBP	1:1	4.8 ± 0.3	5.0 ± 0.1	5.7 ± 0.3	4.15 ± 0.06	7.4 ± 0.3	8.0 ± 0.2	3.94 ± 0.03	5.92 ± 0.09
	1:2	10.0 ± 0.3	10.8 ± 0.1	11.3 ± 0.2	10.2 ± 0.3	13.4 ± 0.2	13.9 ± 0.4		
$CyMe_4$-BTBP	1:1	4.4 ± 0.2	n.d.	6.5 ± 0.2	n.d.	n.d.	5.9 ± 0.1	n.d.	n.d.
	1:2	8.8 ± 0.1		11.9 ± 0.5					

[a] Confidence interval corresponding to $\pm\sigma_{n-1}$, σ_{n-1} being the standard deviation on the mean value of at least three experiments. [b] n.d. = not determined.

Table 2. Stoichiometries (M:L) and Overall Stability Constants (log β)[a] for Other Metal Complexes with C_5-*h*emi-BTP and C_5-BTBP in Methanol ($I = 10^{-2}$ M, Et_4NNO_3; $T = 25$ °C)

	species M:L	Ni^{2+}	Cu^{2+}	Zn^{2+}	Ag^{+}	Pb^{2+}	Cd^{2+}	Hg^{2+}	Tl^{+}
C_5-*hemi*-BTP	1:1		8.7 ± 0.2		5.7 ± 0.2	5.4 ± 0.2			2.3 ± 0.1
	1:2	11.1 ± 0.2	14.7 ± 0.3	11.5 ± 0.3	10.8 ± 0.3		10.7 ± 0.1	11.2 ± 0.2	
C_5-BTBP	1:1		7.2 ± 0.2					5.60 ± 0.02	2.86 ± 0.05
	1:2	11.5 ± 0.1	13.0 ± 0.3	12.3 ± 0.4	9.8 ± 0.2	10.4 ± 0.3	10.8 ± 0.2	11.0 ± 0.1	

[a] Confidence interval corresponding to $\pm\sigma_{n-1}$, σ_{n-1} being the standard deviation on the mean value of at least three experiments.

the constant ionic strength provided by 10^{-2} M Et_4NNO_3. Suprasil quartz cells of 1 cm path length were used. The spectral changes of 2 mL of ligand solutions upon stepwise additions (50 μL) of cationic nitrate solution directly into the measurement cell were recorded from 250 to 370 nm with a Cary 3 (Varian) spectrophotometer. The ligand concentration was in the range $10^{-5}-10^{-4}$ M. The titration was continued to the point where further spectral changes were negligible, the value of the cation to ligand ratio at this point depending upon the stability of the complexes. The data thus obtained were treated with the program Specfit, which uses a factorial analysis to reduce the experimental data (absorbance versus wavelength) and to extract the eigenvalues prior to adjusting the values of the electronic spectra and of the stability constant of the corresponding species with the Marquardt algorithm.[20] Statistical analysis performed by this program allows us to determine the best model.

Microcalorimetry. Microcalorimetric titrations were performed using the 2277 Thermal Activity Monitor Microcalorimeter (Thermometric). Fifteen 15 μL portions of the metal solution were added to the cell containing 2.7 mL of $10^{-4}-10^{-3}$ M ligand solutions in methanol at 25 °C. The heat changes were measured after each addition. Chemical calibration was made by determination of the complexation enthalpy of Rb^+ with 18C6 in methanol.[21] Values of the stability constants (β) and of the enthalpies of complexation (ΔH) were refined simultaneously from these data using the ligand binding analysis program DIGITAM version 4.1[22] and after correction of dilution heat effects determined in separate experiments by adding the metal solutions to 2.7 mL to the pure solvent. The corresponding entropies of complexation (ΔS) were calculated from the expression $\Delta G = \Delta H - T\Delta S$, knowing that $\Delta G = -RT \ln \beta$.

Kinetic Study. The rates of complexation of La^{3+}, Eu^{3+}, and Yb^{3+} with the four ligands were followed by a stopped-flow technique by monitoring the absorbance versus time at a suitable wavelength (according to the system, between 320 and 345 nm; Applied-Photophysics, SX 18MV spectrophotometer). This wavelength was selected on the basis of changes seen in the equilibrium studies. Ligand and Ln(III) solutions prepared in methanol in the presence of Et_4NNO_3 ($I = 10^{-2}$ M) were mixed at 25.0 ± 0.2 °C in a 1 cm optical cell (mixing time 3 ms). The ligand concentration was around 10^{-4} M, and Ln(III) was in sufficient excess to ensure pseudo-first-order conditions ($[Ln^{3+}]_{tot}$ at least 8 times $[ligand]_{tot}$: 8×10^{-4} M < $[Ln^{3+}]_{tot}$ < 5.6×10^{-3} M). Kinetic traces ($A = f(t)$) containing each 1000 points were treated with the program Specfit in order to obtain the value of the observed pseudo-first-order rate constants k_{obs}.[20] Each experiment was carried out at least five times. Variations of k_{obs} with the concentration of Ln^{3+} were fitted to a linear regression. Fisher's F test was used to check the linearity of these curves. The value of the intercept was compared to zero by a Student's t test at the 95% confidence level. The confidence intervals given in Tables 1−6 are the standard deviations obtained from three independent determinations or directly from the least-squares fitting.

Activation parameters (enthalpies $\Delta H^{\ddagger}$ and entropies $\Delta S^{\ddagger}$) were determined for the most interesting systems. The temperature dependence of the rate constants was investigated according to the same protocol described above. A Bioblock Scientific thermostat was used to keep the temperature at different values in the range 20−35 °C (error ±0.2 °C). $\Delta H^{\ddagger}$ and $\Delta S^{\ddagger}$ values of the complexation were determined from the Eyring equation $\ln(k/T) = -\Delta H^{\ddagger}/RT + \Delta S^{\ddagger}/R + \ln(k_B/h)$ plotting $\ln(k/T) = f(1/T)$, with k_B and h, the Boltzmann and Planck constants, respectively.

Table 3. Thermodynamic Parameters[a] of the Formation of the Species (Metal: Ligand) during the Complexation of Eu^{3+} by C_5-BTBP Obtained by Microcalorimetry in Methanol at 25 °C

parameters	1:1	1:2
log β	5.6 ± 0.6 (5.7)[b]	10.5 ± 0.6 (11.3)[b]
$-\Delta G$ (kJ mol^{-1})	32 ± 3	60 ± 3
$-\Delta H$ (kJ mol^{-1})	12 ± 2	28 ± 1
$T\Delta S$ (kJ mol^{-1})	20 ± 5	32 ± 4
ΔS (J mol^{-1} K^{-1})	67 ± 17	107 ± 13

[a] Confidence interval corresponding to $\pm\sigma_{n-1}$, σ_{n-1} being the standard deviation on the mean value of at least three experiments. [b] Spectrophotometric determination.

(20) Gampp, H.; Maeder, M.; Meyer, C. J.; Zueberbuhler, A. D. *Talanta* **1985**, *32*, 95–101. Gampp, H.; Maeder, M.; Meyer, C. J.; Zueberbuhler, A. D. *Talanta* **1985**, *32*, 257–264. Gampp, H.; Maeder, M.; Meyer, C. J.; Zueberbuhler, A. D. *Talanta* **1985**, *32*, 1133–1139. Gampp, H.; Maeder, M.; Meyer, C. J.; Zueberbuhler, A. D. *Talanta* **1986**, *33*, 943–951.

(21) From Thermometric, Experimental and Technical note EN 014b, 2002.

(22) Hallen, D. *Pure Appl. Chem.* **1993**, *65*, 1527–1532.

Table 4. Rate Constants (k_f and k_d)[a] for the Complexation of Lanthanide Cations by C_5-*hemi*-BTP and by *n*-Pr-BTP

lanthanide cation	rate constant	C_5-*hemi*-BTP	*n*-Pr-BTP
La^{3+}	k_f	b	$(182 \pm 5) \times 10^3$ L mol^{-1} s^{-1}
	k_d		318 ± 8 s^{-1}
Eu^{3+}	k_f	$(46.9 \pm 0.6) \times 10^3$ L mol^{-1} s^{-1}	b
	k_d	51.9 ± 0.8 s^{-1}	
Yb^{3+}	k_f	$(7.0 \pm 0.1) \times 10^3$ L mol^{-1} s^{-1}	$(118.7 \pm 0.9) \times 10^3$ L mol^{-1} s^{-1}
	k_d	0.5 ± 0.2 s^{-1}	

[a] Confidence interval corresponding to the standard deviation calculated from the least-squares fitting. [b] Kinetic traces not interpretable.

Table 5. Rate Constants (10^3 L mol^{-1} s^{-1})[a] for the Complexation of Lanthanide Cations with BTBPs

lanthanide cation	C_5-BTBP	$CyMe_4$-BTBP
La^{3+}	223 ± 1	70.5 ± 0.8
Eu^{3+}	27.0 ± 0.3	11.5 ± 0.8
Yb^{3+}	4.07 ± 0.07	1.4 ± 0.1

[a] Confidence interval corresponding to the standard deviation calculated from the least square fitting.

Results and Discussion

Thermodynamic Parameters. A preliminary study of the acid−base behavior of C_5-BTBP and C_5-*hemi*-BTP in methanol using pH-metry provided the protonation constants (log $K_1 = 3.3 \pm 0.1$ for C_5-BTBP, log $K_1 = 5.3 \pm 0.1$ and log $K_2 = 2.8 \pm 0.2$ for C_5-*hemi*-BTP). These values indicate that near neutrality (pH ~8.5 in MeOH), the experimental conditions used for the complexation study, the ligands were unprotonated. The lower basicity of C_5-BTBP compared to C_5-*hemi*-BTP may be explained by the presence of the additional triazine moiety presenting a stronger electron withdrawing character than pyridine.[4]

Complexation in methanol was followed by spectrophotometric titrations of the ligands against the metal ions. The stability constants (β) derived from the spectral changes using the program Specfit are given in Tables 1 and 2.[20]

Microcalorimetry was employed for the complexation of Eu^{3+} with C_5-BTBP to confirm the stoichiometries of the complexes indicated by spectrophotometry and to evaluate the thermodynamic parameters of complexation (ΔG, ΔH, and ΔS). These results are given in Table 3.

***n*-Pr-BTP.** Only small spectral variations were observed in methanol for *n*-Pr-BTP in the presence of La^{3+}. Their interpretation showed the formation of one ML species with a stability constant value close to 10^4 (Table 1). This stoichiometry for La^{3+} was also found with BTP and Me-BTP, but the complexes, studied in methanol/water (0.76/0.24), were less stable (log $\beta = 1.2$ with BTP and 2.2 with Me-BTP).[23] The behavior of this ligand in the presence of the smaller Eu^{3+} and Yb^{3+} cations was different and led to major spectral variations, as shown in Figure 2 for Eu^{3+}. With these two cations, both ML_2 and ML_3 complexes formed. The distribution curves of the species illustrated in Figure 3 in the case of Yb^{3+} shows that the ML_2 complex is always predominant over ML_3. The formation of ML_3 is consistent with both the isolation of such species in the solid state and with solution observations that ML_3 species form only with smaller Ln^{3+} (Sm−Lu), as found in earlier work.[24−29] Note also that both 1:3 and 1:2 stoichiometries have been observed with Eu^{3+} by ESI-MS, consistent with the coexistence of these two species in solution.[30,31] With the larger early lanthanides, the formation of complexes of different natures (M_2L_2, ML, or ML_2) has been reported in structural studies.[32]

For Eu^{3+} and Yb^{3+}, the stability constants of the ML_2 and ML_3 complexes with *n*-Pr-BTP are of the same order of magnitude (log β around 10 for ML_2 and around 14.2 for ML_3). These values are higher than those determined by ESI-MS in a water/methanol (1/1) mixture (log β = 6.7 and 12.0 for ML_2 and ML_3, respectively), in agreement with differences in the solvating properties of the solvents.

C_5-*hemi*-BTP. Marked spectral changes are observed with C_5-*hemi*-BTP in the presence of all the cations studied except La^{3+} and Tl^+. Table 1 presents the stability constants determined for lanthanides and actinides. Unlike *n*-Pr-BTP, this ligand forms only ML species, as observed with terpy, showing chemical properties similar to those of *hemi*-BTP.[23] This stoichiometry is consistent with that determined previously by liquid−liquid extraction and by X-ray crystallography.[33] The stability constant values (log β) increase in the series of lanthanides from 2.8 for La^{3+} to 4.19 for Yb^{3+}. This variation may be attributable to the increase of the charge density of the cations in the series due to the lanthanide contraction. The tetravalent thorium cation and the divalent uranyl also form 1:1 complexes which are almost as stable as that of Gd^{3+}.

With first-row transition-metal cations (Table 2), the results show the formation of stable 1:2 complexes and of an additional ML complex with Cu^{2+}. The stability constant values for the ML_2 species follow the Irving−Williams rule, with a maximum of stability for the copper complex.[34] The results in Table 2 for some other heavy-metal cations show the formation of both ML and ML_2

(23) Ionova, G.; Rabbe, C.; Guillaumont, R.; Ionov, S.; Madic, C.; Krupa, J.-C.; Guillaneux, D. *New J. Chem.* **2002**, *26*, 234–242. François, N. Ph.D. Thesis, Université Henri Poincaré, Nancy I, France, **1999** (CEA-R-5902, 2000).

(24) Drew, M. G. B.; Guillaneux, D.; Hudson, M. J.; Iveson, P. B.; Russel, M. L.; Madic, C. *Inorg. Chem. Commun.* **2001**, *4*, 12–15.

(25) Kolarik, Z.; Müllich, U.; Gassner, F. *Solv. Extr. Ion Exch.* **1999**, *17*, 23–32.

(26) Denecke, M. A.; Rossberg, A.; Panak, P. J.; Weigl, M.; Schimmelpfennig, B.; Geist, A. *Inorg. Chem.* **2005**, *44*, 8418–8425.

(27) Drew, M. G. B.; Hudson, M. J.; Iveson, P. B.; Madic, C.; Russel, M. L. *J. Chem. Soc., Dalton Trans.* **2000**, 2711–2720.

(28) Denecke, M. A.; Panak, P. J.; Burdet, F.; Weigl, M.; Geist, A.; Klenze, R.; Mazzanti, M.; Gompper, K. *C. R. Chem.* **2007**, *10*, 872–882.

(29) Iveson, P. B.; Rivière, C.; Guillaneux, D.; Nierlich, M.; Thuery, P.; Ephritikhine, M.; Madic, C. *Chem. Commun.* **2001**, 1512–1513.

(30) Colette, S.; Amekraz, B.; Madic, C.; Berthon, L.; Cote, G.; Moulin, C. *Inorg. Chem.* **2002**, *41*, 7031–7041.

(31) Colette, S.; Amekraz, B.; Madic, C.; Berthon, L.; Cote, G.; Moulin, C. *Inorg. Chem.* **2003**, *42*, 2215–2226.

(32) Drew, M. G. B.; Guillaneux, D.; Hudson, M. J.; Iveson, P. B.; Madic, C. *Inorg. Chem. Commun.* **2001**, *4*, 462–466.

(33) Hudson, M. J.; Drew, M. G. B.; Foreman, M.R.StJ.; Hill, C.; Huet, N.; Madic, C.; Youngs, T. G. A. *Dalton Trans.* **2003**, 1675–1685.

(34) Irving, H.; Williams, R. J. P. *J. Chem. Soc.* **1953**, 3192–3210.

Table 6. Activation Enthalpy and Entropy for the Formation ($\Delta H_f^{\ddagger}$, $\Delta S_f^{\ddagger}$) and Dissociation ($\Delta H_d^{\ddagger}$, $\Delta S_d^{\ddagger}$) of Different Complexes (Methanol; $I = 10^{-2}$ M, Et_4NNO_3)

	$\Delta H_f^{\ddagger}$ (kJ mol^{-1})	$\Delta S_f^{\ddagger}$ (J mol^{-1} K^{-1})	$\Delta H_d^{\ddagger}$ (kJ mol^{-1})	$\Delta S_d^{\ddagger}$ (J mol^{-1} K^{-1})
C_5-*hemi*-BTP (Eu^{3+})	51 ± 2	16 ± 3	43 ± 2	−70 ± 4
n-Pr-BTP (Yb^{3+})	44 ± 1	1 ± 2		
C_5-BTBP (La^{3+})	39 ± 1	−9 ± 2		
C_5-BTBP (Eu^{3+})	50 ± 1	9 ± 2		

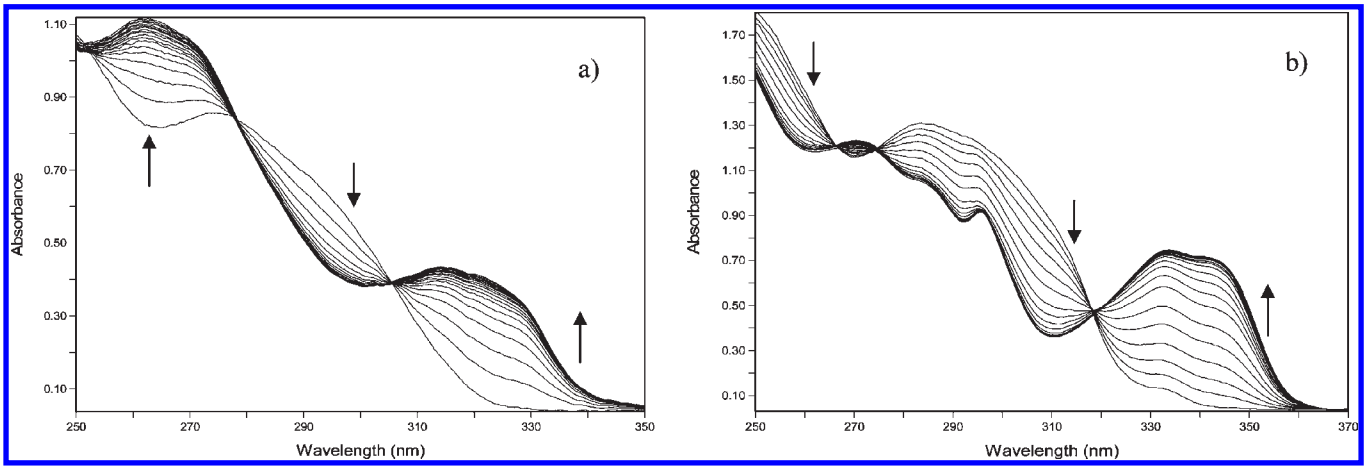

Figure 2. Spectral variations corresponding to the complexation in methanol at 25 °C of (a) Eu^{3+} with *n*-Pr-BTP ($C_L = 5 \times 10^{-5}$ M; $0 \le R = C_M/C_L \le 1.7$) and of (b) Yb^{3+} with C_5-BTBP ($C_L = 10^{-5}$ M; $0 \le R = C_M/C_L \le 2.2$). $I = 10^{-2}$ M Et_4NNO_3.

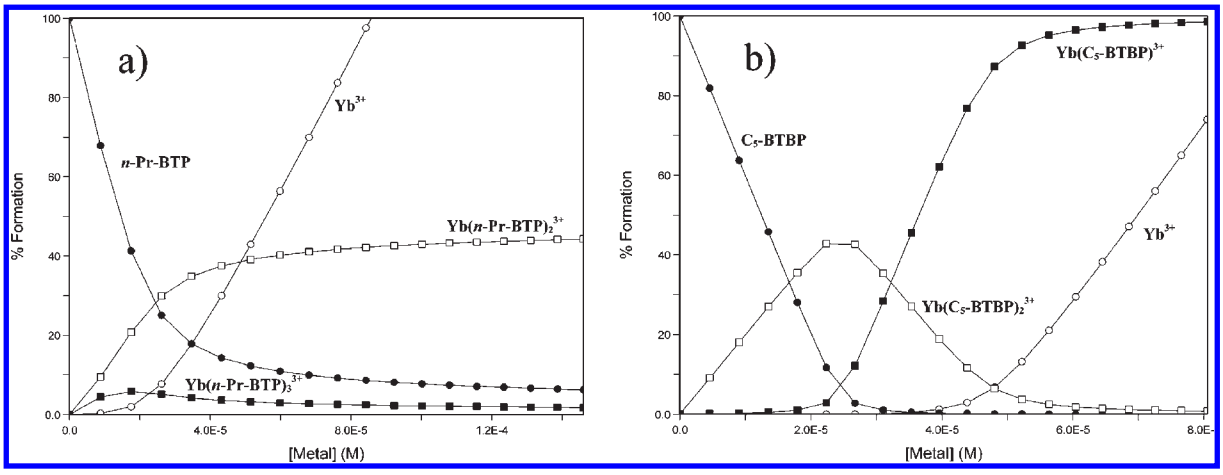

Figure 3. Distribution curves of all the species present in the systems (a) Yb^{3+}/*n*-Pr-BTP and (b) Yb^{3+}/C_5-BTBP in methanol at 25 °C ($C_L = 10^{-5}$ M).

complexes with Ag^+ and of single complexes with Pb^{2+} (ML) and with Cd^{2+} and Hg^{2+} (ML_2). The two ML complexes with Ag^+ and Pb^{2+} have almost the same stabilities (log β about 5.5), as do the three ML_2 complexes with Ag^+, Cd^{2+}, and Hg^{2+} (log β about 11). Tl^+ forms a ML complex of lower stability (log $\beta = 2.3$).

BTBPs. Complexation of lanthanides with the two ligands C_5-BTBP and $CyMe_4$-BTBP in methanol led in all cases to major spectral variations involving one or several isosbestic points. The example of Yb^{3+} with C_5-BTBP is presented in Figure 2.

With C_5-BTBP, the interpretation of the spectrophotometric data shows the formation of both ML and ML_2 species with all the lanthanides (Table 1). As with C_5-*hemi*-BTP, the increase of the complex stability in the series ($\Delta \log \beta = 3.2$ and 3.9 from La^{3+} to Yb^{3+}, for ML and ML_2 complexes, respectively) is consistent with the increase of the cationic charge density/polarizing power along the series. Except for Eu^{3+}, Er^{3+}, and Yb^{3+}, a positive cooperative effect for the formation of ML_2 complexes is observed for all the Ln(III) species (Δ = log β(ML_2 complex) − 2 log β(ML complex) = 0.4 − 1.9). Only one ML complex is formed with the two actinides, the most stable one being obtained with UO_2^{2+} (log $\beta = 5.92$). This stoichiometry for Th^{4+} and UO_2^{2+} is consistent with previous extraction results.[35] The better affinity of C_5-BTBP with the linear UO_2^{2+} in comparison to the case for C_5-*hemi*-BTP could be explained by the structure and number of N-donor atoms,

(35) Retegan, T.; Ekberg, C.; Dubois, I.; Fermvik, A.; Skarnemark, G.; Wass, T. J. *Solv. Extr. Ion Exch.* **2007**, *25*, 417–431.

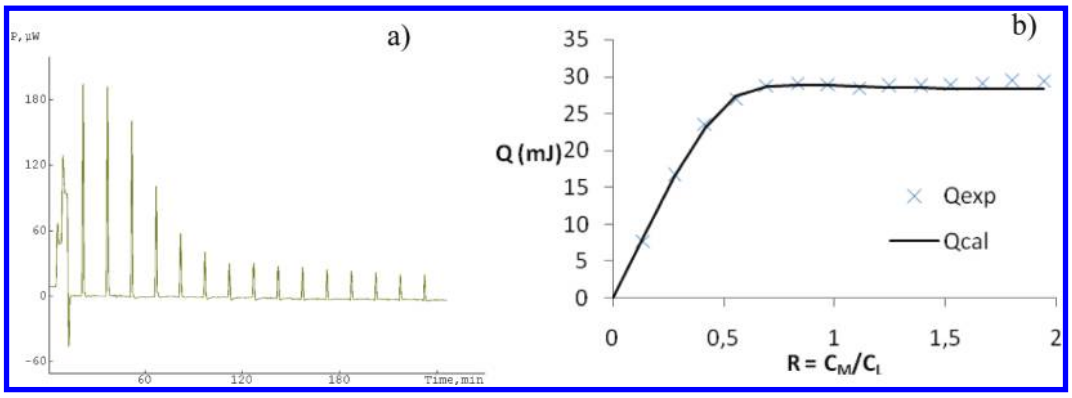

Figure 4. Microcalorimetric titration of C_5-BTBP by Eu^{3+}: (a) thermogram corresponding to the heat evolved during each addition of Eu^{3+} in the C_5-BTBP solution; (b) experimental and calculated variations of the heat of complexation versus the metal to ligand concentration ratio, *R*.

which are different for these two ligands and are more favorable in the case of BTBP. With Th^{4+}, which possesses a higher charge, the complex stability is weaker than with Ln^{3+} and can be explained in term of important solvation effects.

In the case of $CyMe_4$-BTBP, once again two species ML and ML_2 are formed with La^{3+} and Eu^{3+}. The stability constants are higher for the Eu^{3+} complexes in comparison to those of La^{3+} and follow the trend observed in liquid−liquid extraction into octanol, for which better distribution ratios have been found for lanthanide cations in the middle to the end of the series.[7] With Yb^{3+}, only an ML species is formed, of stability intermediate between those of the ML complexes with La^{3+} and Eu^{3+}. No great difference of complex stability as a function of the nature of the substituent on the BTBP is observed except for Yb^{3+}, which forms a more stable ML complex with C_5-BTBP ($\log\beta_{11} = 8.0$) than with $CyMe_4$-BTBP ($\log\beta_{11} = 5.9$).

With these two ligands, the distribution curves of the species show that, beyond the ratio $R = C_M/C_L$ of 3.5, ML is predominant, as illustrated in Figure 3 in the case of Yb^{3+} with C_5-BTBP. This is in agreement with earlier work on several BTBP ligands, including C_5-BTBP and $CyMe_4$-BTBP, in the solid state, in solution as studied by NMR titrations, and in biphasic media.[5−9,36]

The complexation of Eu^{3+} with C_5-BTBP was studied in methanol using microcalorimetry in order to determine the enthalpy (ΔH) and the free energy (ΔG) of complexation. The thermogram obtained and the corresponding plot of the heat exchanged *Q* (mJ) versus the concentration ratio *R* of metal to ligand are presented in Figure 4. The presence of a break point at $R = 0.55$ on the latter curve clearly indicates the formation of a ML_2 complex. The results obtained from these data (Table 3) confirm the stoichiometry of the complexes deduced from spectrophotometric measurements. There is also an excellent agreement between the values of the stability constants obtained by both techniques. The formation of the ML complex is both enthalpically and entropically driven (positive $T\Delta S$ and negative ΔH values). The positive entropy may be due to an increase of the disorder due to the displacement of solvent molecules by the ligand, and the exothermic effect can be related to the strength of the cation−ligand interaction. The formation of the ML_2 complex is characterized by an enthalpy change ($-\Delta H = 16$ kJ mol^{-1}), which is slightly greater than the entropy change ($T\Delta S = 12$ kJ mol^{-1}). This suggests that the metal−ligand interaction dominates desolvation effects.

The binding properties of C_5-BTBP toward transition- and various heavy-metal cations were also investigated. Spectral variations were similar to those obtained with Ln(III), Th^{4+}, and UO_2^{2+}. The nature of the complexes formed and their stability constants are given in Table 2. Complexes of the same stoichiometries (ML_2 in all cases with an additional ML species with copper) were found with the three transition-metal cations as with the C_5-*hemi*-BTP. The stability constants are similar for both ligands, except for the ML complex with Cu^{2+}, which is slightly less stable ($\Delta\log\beta = 1.5$). The most stable ML_2 complex is observed with Cu^{2+}, for which high distribution ratios have been determined.[11] Stoichiometries of heavy-metal complexes with C_5-BTBP are different from those observed for C_5-*hemi*-BTP. The results show the formation of only ML_2 complexes of similar stability with Ag^+, Pb^{2+}, and Cd^{2+}. For Hg^{2+}, the ML_2 complex is also formed with an additional ML species. As for C_5-*hemi*-BTP, C_5-BTBP forms a weak ML complex with Tl^+.

Kinetic Data. The kinetics of complexation of La^{3+}, Eu^{3+}, and Yb^{3+} with the four ligands was followed by the stopped-flow technique under pseudo-first-order conditions. The absorbance at a wavelength corresponding to the maximum overall change was monitored versus time for different concentrations of Ln(III). The values of activation parameters $\Delta H^{\ddagger}$ and $\Delta S^{\ddagger}$ obtained for the most representative systems are summarized in Table 6. Figure 8 shows the Eyring plots for the formation and dissociation of the C_5-*hemi*-BTP/Eu^{3+} complex. The linear temperature dependence obtained in all cases proves the validity of the Eyring equation.

C_5-*hemi*-BTP and *n*-Pr-BTP. The time dependence of the absorbance could be well fitted by a single-exponential function. The example of C_5-*hemi*-BTP with Yb^{3+} is illustrated in Figure 5. The excellent linear dependence of $\ln(A_{inf} - A)$ with time confirms the first-order process of the reaction. The variation of the absorbance measured on the experimental kinetic traces was in agreement with those of the equilibrium measurements. Studies of the complexation of La^{3+} with C_5-*hemi*-BTP and of Eu^{3+} with *n*-Pr-BTP were not possible due to the negligible absorbance changes in the case of La^{3+} and the rapidity of the reaction in the case of Eu^{3+}.

(36) Foreman, M. R. S.; Hudson, M. J.; Drew, M. G. B.; Hill, C.; Madic, C. *Dalton Trans.* **2006**, 1645–1653.

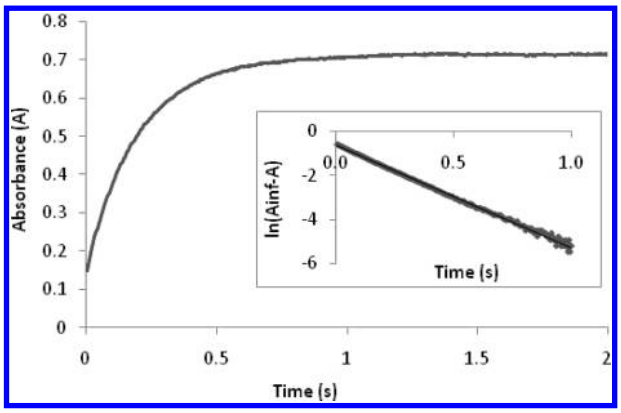

Figure 5. Experimental kinetic trace recorded for the complexation of Yb^{3+} ($C_M = 1.37 \times 10^{-3}$ M) with C_5-*hemi*-BTP ($C_L = 1.14 \times 10^{-4}$ M) at $\lambda = 326$ nm in methanol. $T = 25$ °C, and $I = 10^{-2}$ M Et_4NNO_3. The insert gives a logarithmic graph versus time (A_{inf} and A: absorbances at the end and at any time of measurement, respectively).

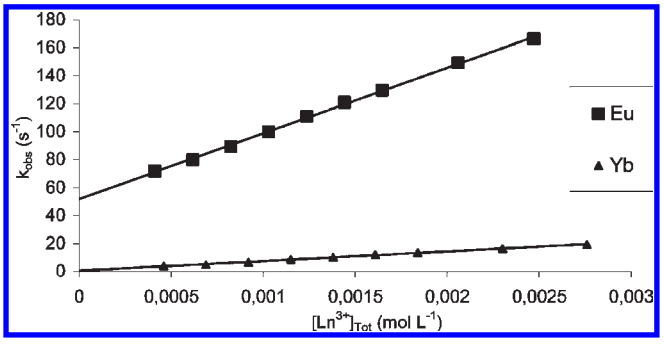

Figure 6. Observed pseudo-first-order rate constants (k_{obs}) as a function of the total metal ion concentration for the complexation with C_5-*hemi*-BTP in methanol at 25 °C.

The overall reactions of complexation of Eu^{3+} and Yb^{3+} with C_5-*hemi*-BTP and of La^{3+} with *n*-Pr-BTP can be expressed by the equilibrium

$$Ln^{3+} + L \underset{k_d}{\overset{k_f}{\rightleftarrows}} LnL^{3+}$$

The observed pseudo-first-order rate constants (k_{obs}) vary linearly with $[Ln^{3+}]_{tot}$, the concentration of Ln^{3+} (La^{3+}, Eu^{3+}, Yb^{3+}) (Figures 6 and 7), with a nonzero intercept, according to the expression

$$k_{obs} = k_f[Ln^{3+}]_{tot} + k_d$$

The formation (k_f) and the dissociation (k_d) rate constant values could be calculated from the slope and intercept of these curves, respectively (Table 4).

With C_5-*hemi*-BTP, the highest values are found for the complexation of Eu^{3+}. In this case, the fact that k_d values are not negligible with regard to k_f could explain why the Eu^{3+} complex (log $\beta = 3.6$) is less stable than the Yb^{3+} complex (log $\beta = 4.19$). Good agreement exists between these thermodynamic values and those calculated from the ratio of the rate constants k_f and k_d (log (k_f/k_d) = 3.0 for Eu^{3+} and 4.15 for Yb^{3+}). Eyring plots determined for the C_5-*hemi*-BTP/Eu^{3+} system are presented in Figure 8. Table 6 shows that the activation enthalpies for the formation and the dissociation of this complex are both positive with a slightly higher value for the formation step ($\Delta H_f^{\ddagger} = 51$ kJ mol^{-1} and $\Delta H_d^{\ddagger} = 43$ kJ mol^{-1}). In contrast, the activation

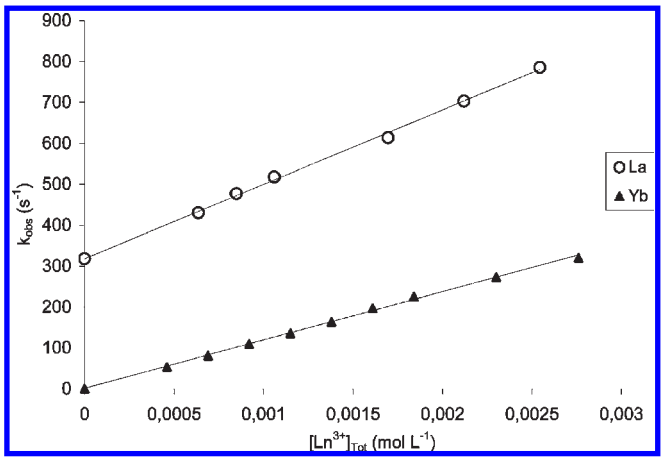

Figure 7. Observed pseudo-first-order rate constants (k_{obs}) as a function of the total metal ion concentration for the complexation with *n*-Pr-BTP in methanol at 25 °C.

entropy values are different ($\Delta S_f^{\ddagger} = 16$ J mol^{-1} K^{-1} and $\Delta S_d^{\ddagger} = -70$ J mol^{-1} K^{-1}) and suggest an entropically driven equilibrium ($\Delta\Delta S^{\ddagger} = 86$ J mol^{-1} K^{-1}). A good agreement was found between the value of the stability constant (log $\beta = 3.1$) calculated from these activation parameters at 25.0 and that determined by UV absorption spectrophotometry (log $\beta = 3.6$).

In the case of *n*-Pr-BTP with Yb^{3+}, where a nonsignificant intercept was observed, only the value of k_f was determined. The difference between the absorbance value observed on the experimental kinetic traces at $t = 0$ and the value calculated from the absorption spectra is in agreement with a fast pre-equilibrium for the formation of the Yb(*n*-Pr-BTP)$^{3+}$ species followed by further binding of the ligand to the cation:

$$Yb^{3+}{}_{solvated} + n\text{-Pr-BTP} \rightleftarrows Yb(n\text{-Pr-BTP})^{3+}{}_{outer\ sphere\ complex}$$

$$Yb(n\text{-Pr-BTP})^{3+}{}_{outer\text{-}sphere\ complex} \underset{k_d}{\overset{k_f}{\rightleftarrows}} Yb(n\text{-Pr-BTP})^{3+}{}_{inner\text{-}sphere\ complex}$$

$$Yb(n\text{-Pr-BTP})^{3+} + n\text{-Pr-BTP} \rightleftarrows Yb(n\text{-Pr-BTP})_2{}^{3+}$$

$$Yb(n\text{-Pr-BTP})_2{}^{3+} + n\text{-Pr-BTP} \rightleftarrows Yb(n\text{-Pr-BTP})_3{}^{3+}$$

Since water molecules are bound to the lanthanide cation and all species are solvated, the Eigen−Wilkins mechanism could be plausible, for the reaction involves first the formation of an intermediate outer-sphere complex in which Yb^{3+} and *n*-Pr-BTP are separated by one or more solvent molecules. The release of these solvent molecules leads then to the formation of the inner-sphere complex Yb(*n*-Pr-BTP)$^{3+}$ followed by the binding of a second and then a third ligand molecule to form Yb(*n*-Pr-BTP)$_2{}^{3+}$ and Yb(*n*-Pr-BTP)$_3{}^{3+}$.[37] This assumption is based on spectrophotometrical results and on the kinetics traces. Considering the distribution curve (Figure 3) showing the predominance of ML_2 over ML_3 species, the formation of Yb(*n*-Pr-BTP)$_3{}^{3+}$ should not be favorable under the conditions used in the

(37) Eigen, M.; Wilkins, R. G. *Adv. Chem. Ser.* **1965**, *49*, 55–67.

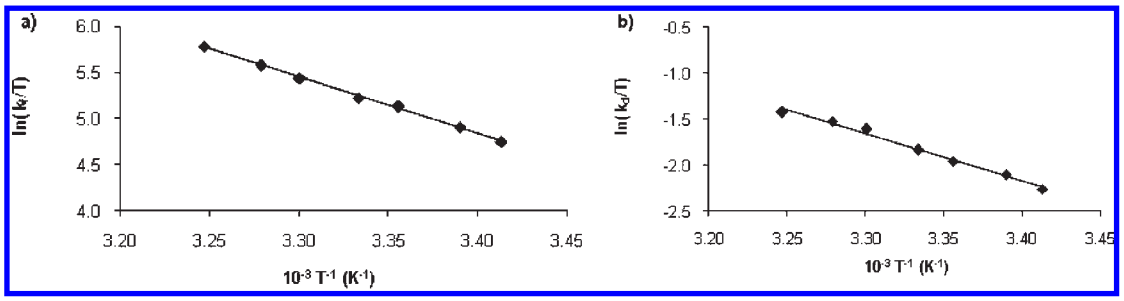

Figure 8. Eyring plot obtained for the (a) formation and (b) dissociation of the C_5-*hemi*-BTP/Eu^{3+} complex.

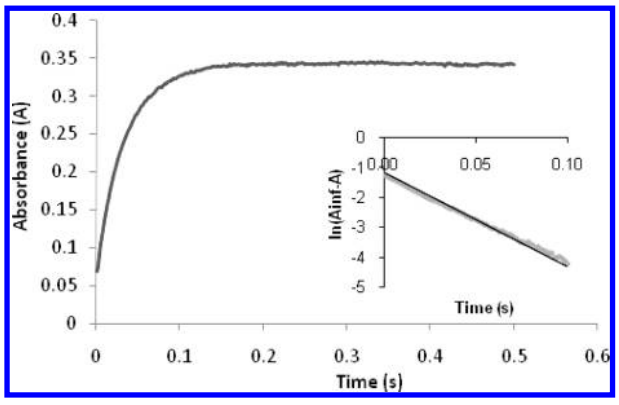

Figure 9. Experimental kinetic trace recorded for the complexation of La^{3+} ($C_M = 9.09 \times 10^{-4}$ M) with $CyMe_4$-BTBP ($C_L = 1.07 \times 10^{-4}$ M): $\lambda = 345$ nm in methanol, $T = 25$ °C, and $I = 10^{-2}$ M Et_4NNO_3. The insert gives a logarithmic graph versus time (A_{inf} and A are absorbances at the end and at any time of measurement, respectively).

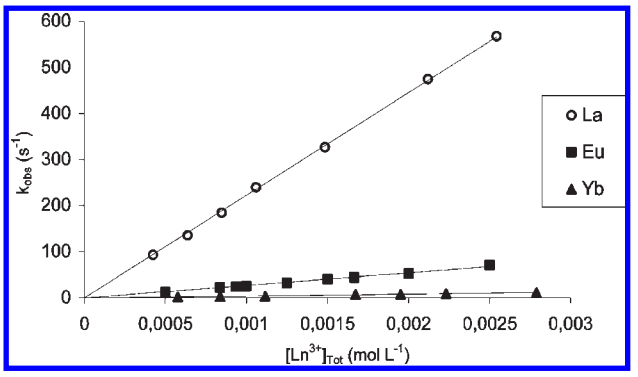

Figure 10. Observed pseudo-first-order rate constants (k_{obs}) as a function of the total metal ion concentration for the complexation with C_5-BTBP in methanol at 25 °C.

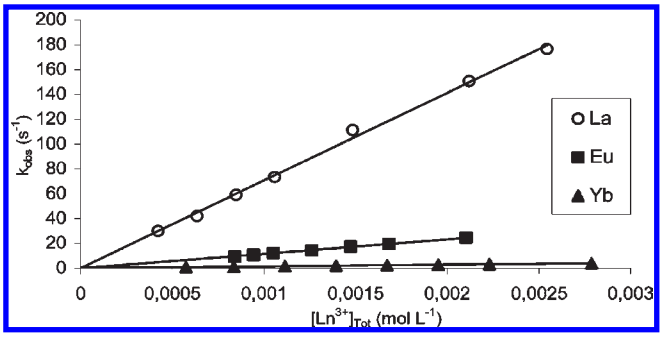

Figure 11. Observed pseudo-first-order rate constants (k_{obs}) as a function of the total metal ion concentration for the complexation with $CyMe_4$-BTBP in methanol at 25 °C.

kinetic study and thus is assumed not to have contributed to the changes. Experiments performed with an excess of ligand showed a linear dependence of the observed pseudo-first-order rate constants with the ligand concentration with a slope value similar to that obtained in the experiments carried out in the presence of an excess of metal. These results suggest that the rate constant (Table 4) should correspond to the rate of the formation of Yb(*n*-Pr-BTP)$^{3+}$, which would be the rate-determining step. The activation enthalpy for this reaction is positive and is lower than that obtained for the C_5-*hemi*-BTP/Eu^{3+} complex ($\Delta H_f^{\ddagger} = 44$ and 51 kJ mol^{-1}, respectively). For this system, the activation entropy value is near zero (Table 6).

BTBPs. As for the BTP ligands, the variations of the absorbance versus time recorded in the case of C_5-BTBP and $CyMe_4$-BTBP were fitted with a single-exponential function. The first-order nature of the reactions is shown by the good linear dependence of $\ln(A_{inf} - A)$ on time. The experimental kinetic trace measured for the formation of the La^{3+} complexes with $CyMe_4$-BTBP is presented in Figure 9.

The values of pseudo-first-order rate constants (k_{obs}) obtained for different concentrations of metal ion were calculated from the kinetic traces. In all cases, these values vary linearly with the metal concentration and the plots pass through the origin (Figures 10 and 11).

Linear regression analysis provided the rate constants for the formation of lanthanide complexes with these two ligands (Table 5). For both, the rate constants decrease across the series, which could be due to the stronger solvation of the cations of the end of the series as observed for hydration.[38]

In addition, rate constants are always lower with $CyMe_4$-BTBP than with C_5-BTBP, suggesting slower complex formation when bulkier substituents are present.

The kinetic measurements are consistent with a single rate-determining step, though clearly there must be at least three steps in the formation of ML_2:

$$Ln^{3+}{}_{solvated} + BTBP \rightleftarrows Ln(BTBP)^{3+}{}_{outer\text{-}sphere\ complex}$$

$$Ln(BTBP)^{3+}{}_{outer\text{-}sphere\ complex} \underset{k_d}{\overset{k_f}{\rightleftarrows}} Ln(BTBP)^{3+}{}_{inner\text{-}sphere\ complex}$$

$$Ln(BTBP)^{3+} + BTBP \rightleftarrows Ln(BTBP)_2{}^{3+}$$

In the case of the BTBPs, as for *n*-Pr-BTP with Yb^{3+}, the value of the initial absorbance in the kinetic traces was

(38) Marcus, Y. *Ion Properties*; Marcel Dekker: New York, 1997.

different from that determined from the absorption spectra. The formation of an outer-sphere complex also presumably intervenes before the formation of the $Ln(BTBP)^{3+}$ species, although it is assumed that this would be too fast a process to be followed by simple stopped-flow measurements. It is possible that the rate constants (Table 5) correspond to the rate of the rearrangement of the outer-sphere complex, leading to the formation of $Ln(BTBP)^{3+}_{\text{inner-sphere complex}}$ species. This assumption was supported by a a linear dependence of $\ln(A_{inf} - A)$ with time confirming the first-order kinetics traces performed under second-order conditions. The zero intercept means that in these conditions the rate constant for the back reaction (k_d) was negligible. As shown in the distribution curves (example in Figure 3), under the kinetic experimental conditions (excess of metal), the formation of $Ln(BTBP)_2^{3+}$ is undetectable, $Ln(BTBP)^{3+}$ being the predominant species. Activation enthalpies and entropies were calculated for the formation of La^{3+} and Eu^{3+} complexes with C_5-BTBP. Significantly different values of activation parameters were found with these two cations (Table 6). The enthalpy value is greater for Eu^{3+} ($\Delta H_f^{\ddagger} = 50$ kJ mol^{-1}) than for La^{3+} ($\Delta H_f^{\ddagger} = 39$ kJ mol^{-1}), which is consistent with the faster kinetics observed for La^{3+} and the lower solvation of this cation. Formation of both complexes leads to low activation entropies: negative for La^{3+} and positive for Eu^{3+} (Table 6).

Conclusions

Thermodynamic and kinetic aspects of the complexation of *n*-Pr-BTP, C_5-*hemi*-BTP, C_5-BTBP, and $CyMe_4$-BTBP toward several cations were investigated in a homogeneous medium. The results obtained using absorption spectrophotometry and microcalorimetry showed different stoichiometries and stability constants depending on the ligand and the cation. The stoichiometries are consistent with those obtained in previous works in biphasic media and in the solid state. The higher stability constants observed for the lanthanides near the end of the series (Er^{3+} and Yb^{3+}) with all the ligands are attributed to the more important charge density of these cations. The high affinity of C_5-*hemi*-BTP and C_5-BTBP for transition- and other heavy-metal cations makes these cations potential competitors with lanthanides and actinides in industrial separation processes.

The rapid kinetics study provided further information on the rate of the complexation of lanthanides with these four ligands and hence a better understanding of the recognition process and possible mechanisms in which inner-sphere complexes are formed. The results showing faster reaction in homogeneous medium than in biphasic medium emphasize the important role of interfacial phenomena in liquid−liquid extraction with these ligands.

Acknowledgment. Financial support from the integrated European project EUROPART (contract FI6W-CT-2003-508854) and the French Group of Researches GdR PARIS is gratefully acknowledged. We thank Dr. Mark Foreman and Dr. Michael Hudson for providing the ligands and Dr. Pierre Jost for helpful suggestions.